Youssef Ouhassan
Ibn Tofail University
Faculty of Sciences
Kenitra
Morocco

Seddik Bri
Full Professor
Group MIN
Superior School of Technology
Moulay Ismail University - Meknes
Morroco

My Chrif El boubakraoui
Full Professor
Superior School of Technology
Moulay Ismail University - Meknes
Morroco

Mohamed Habibi
Full Professor
Ibn Tofail University
Faculty of Sciences
Kenitra
Morroco

Dielectric Properties of Ceramic Composite Materials Based on Alumina Reinforced by Titanium Carbide

The aim of this research work is to study the dielectric and microwave properties of the three ceramic composites Al_2O_3-TiC, Al_2O_3-0.3TiC and Al_2O_3-0.7TiC. The results obtained show that the effective permittivity increases with the increase in the filling rate of titanium carbide TiC inclusions and their contrasts. As for the classical mixing laws, they make it possible to estimate permittivity for low volume fractions and low contrasts. The values of the real part of the complex permittivity decrease with frequency increase in the two bands X and Ku, while the imaginary part is approximately constant in the X band and takes negative values in the Ku band.

Keywords: *Dielectric constant, Dielectric properties, Rectangular waveguide, TiC, Mixing laws, Microwaves, Finite element method.*

1. INTRODUCTION

The knowledge of the dielectric properties of materials is crucial in various fields of research, such as materials science, microwave circuit design, absorber development and in many engineering applications [1]. As well as the many problems of radio wave propagation and their applications in remote sensing depend on the correct values of these properties [2]. These properties are important for food applications [3], telecommunications [1, 4] and civil engineering [5]. Several methods have been developed in order to extract these properties. We distinguish various methods: resonant [6], free space [7], capacitive [8], transmission lines [9]. The transmission line method offers broadband characterization [10]. While the resonant method is narrow band and the free space method is less precise [11]. The addition of Titanium carbide (TiC) particles distributed in a homogeneous way in the Al_2O_3 alumina matrix makes it possible to obtain a ceramic composite material Alumina titanate (Al_2O_3-TiC) with effective absorption properties of electromagnetic waves at high temperatures [12] as well as improved electrical conductivity [13]. Recently, these microwave absorbing materials have attracted the attention of researchers for applications in electronic devices and microwave absorbing [14, 15].

The aim of this work is to study, on the one hand, the impact of the filling rate of the inclusions of titanium carbide TiC on the effective permittivity of Al_2O_3-TiC composite, and on the other hand the microwave characterization of the three ceramic composites Al_2O_3-TiC, Al_2O_3-0.3TiC and Al_2O_3-0.7TiC in both X and Ku bands, using the transmission / reflection (T/R) method.

Received: April 2020, Accepted: June 2020
Correspondence to: Youssef Ouhassan
Faculty of Sciences, Laboratory of Electrical Engineering and Energy Systems, Ibn tofail, Morocco,
E-mail: ouhassan.youssef@gmail.com
doi:10.5937/fme2004908O
© Faculty of Sciences, Kenitra. All rights reserved

2. THEORETICAL STUDY

2.1 Mixing laws

In a heterogeneous medium, when the size of the heterogeneities is small compared to the wavelength λ of the signal, the medium can be represented by an effective permittivity ε_{eff} [16].Several laws have been proposed in the literature for predicting the effective permittivity of a non-homogeneous material if the properties of the different phases that constitute it are known. In this section, we briefly present some of the most widely used laws.

Maxwell-Garnett's law has been applied to isolated spherical inclusions, dispersed in a matrix [17]. The effective permittivity ε_{eff} in a three dimensional 3D can be calculated by the following equation:

$$\varepsilon_{eff} = \varepsilon_1 + 3f\varepsilon_1 \frac{\varepsilon_2 - \varepsilon_1}{\varepsilon_2 + 2\varepsilon_1 - f(\varepsilon_2 - \varepsilon_1)} \quad (1)$$

where f is the volume fraction. ε_1 and ε_2 are the permittivities of the matrix and inclusions respectively.

Another theory has been proposed by Bruggeman is given by the relation:

$$(1-f)\frac{\varepsilon_1 - \varepsilon_{eff}}{\varepsilon_1 + \varepsilon_{eff}} + f\frac{\varepsilon_2 - \varepsilon_{eff}}{\varepsilon_2 + \varepsilon_{eff}} = 0 \quad (2)$$

These two laws are strictly valid for the cases of spherical and isolated particles. Lichteneker and Rother have proposed an alternative given by the following relation:

$$\ln(\varepsilon_{eff}) = f\ln(\varepsilon_2) + (1-f)\ln\varepsilon_1 \quad (3)$$

In this case, the geometry of the inclusions does not have an important role in determining the macroscopic dielectric behavior of the mixture.

Looyenga has developed another interesting equation, which can be written in the following form:

$$\varepsilon_{eff} = \left[\varepsilon_1^{1/h} + f(\varepsilon_2^{1/h} - \varepsilon_1^{1/h}) \right]^h \quad (4)$$

For spherical inclusions h = 3, the effective permittivity ε_{eff} can be written in the following form:

$$\varepsilon_{eff} = \left[\varepsilon_1^{1/3} + f(\varepsilon_2^{1/3} - \varepsilon_1^{1/3} \right]^3 \quad (5)$$

For h = ± 1, we find the Wiener terminals. The value of ε_{eff} is given by the two equations:

$$\varepsilon_{eff\perp} = \frac{\varepsilon_2 \varepsilon_1}{f\varepsilon_1 + (1-f)\varepsilon_2} \quad (6)$$

$$\varepsilon_{eff\parallel} = f\varepsilon_2 + (1-f)\varepsilon_1 \quad (7)$$

The finite element method (FE) [18 ,19] is used to calculate the complex effective permittivity of composite materials. This permittivity is obtained by calculating the spatial distribution of the local potential within the computational domain as shown in Figure 2 by solving the following Laplace equation:

$$\nabla(\varepsilon_0 \varepsilon(r) \nabla V) = 0 \quad (8)$$

where ε (r) and V are the local relative permittivity and the potential distribution inside the spatial domain respectively with zero charge density.
$\varepsilon_0 = 8.85 \times 10^{-12}$ Farad / m is the permittivity of the vacuum.

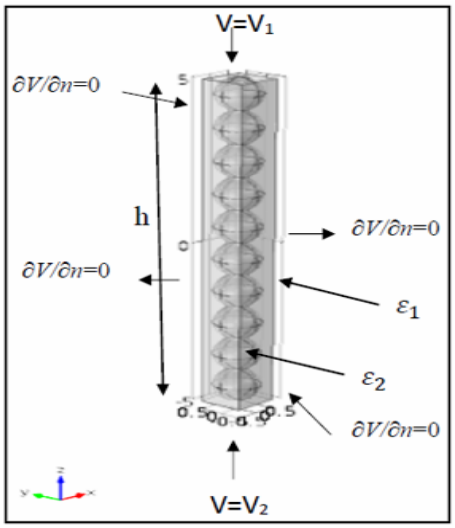

Figure 1. Unit cell of the composite material studied and boundary conditions

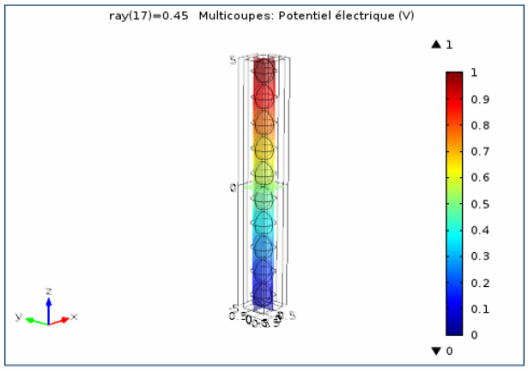

Figure 2. Spatial distribution of the electric field

The unit cell of the composite studied, which has dimensions of (1x1x10) mm^3, is filled with a composite dielectric, statistically isotropic, composed of two materials with complex dielectric constants ε_1 and ε_2 as shown in Figure 1. The material is exposed to a static electric field that is generated by a potential difference (V_1-V_2 = 1 V) between the opposite faces of the unit cell [17]. By imposing periodic boundary conditions ∂V / ∂n = 0 on the planes parallel to the direction (Oz). The effective permittivity ε_{eff} is calculated from the energy W stored in the capacitor [19]:

$$W = \frac{1}{2} \varepsilon_0 \varepsilon_{eff} \frac{S}{h} (V_1 - V_2)^2 \quad (9)$$

where V_1-V_2=1V is the potential difference applied to the upper and lower planes of the unit cell of area S and h is the distance between the two planes.

2.2 Proposed microwave technique

The microwave technique used is a characterization in transmission/reflection (T/R) [20], based on the extraction of the [S_{ij}] parameters. This technique involves placing the material sample under test (MUT) inside the rectangular waveguide and calculating the Sij parameters. The only dominant fundamental mode TE_{10} propagates inside the waveguide and the sample is precisely adjusted by the location of the in sample port. The corresponding transmission matrices M_a and M_b are calculated from the following equation [21 ,22]:

$$M_n = \frac{1}{S_{21n}} \begin{pmatrix} S_{12n}S_{21n} - S_{11n}S_{22n} & S_{11n} \\ -S_{22n} & 1 \end{pmatrix} \quad (10)$$

with n = a or b
M_a: corresponds to the compute cell which is empty or partially filled by a dielectric whose complex permittivity is known with precision on the frequency band studied.
M_b: corresponds to the compute cell partially filled by the sample to be characterised the material under test (MUT).
M_a and M_b can also be written as a product of five matrices:

$$\begin{cases} M_a = x.T_{ref\,a}.T_a.T_{ref\,a}^{-1}.y \\ M_b = x.T_{ref\,b}.T_b.T_{ref\,b}^{-1}.y \end{cases} \quad (11)$$

where:
• x and y are the error matrices assumed to be unchanged during the two calculations.
• $T_{ref\,n}$ is the transmission matrix corresponding to the impedance jump at the Air/Material interface (Air/sample/Air) causing reflections of the electromagnetic wave, including the transmission matrix.

$$T_{ref\,n} = \begin{pmatrix} \frac{1}{1-\Gamma_n} & \frac{\Gamma_n}{1-\Gamma_n} \\ \frac{\Gamma_n}{1-\Gamma_n} & \frac{1}{1-\Gamma_n} \end{pmatrix} \quad (12)$$

$$\Gamma_n = \frac{\gamma_0 - \gamma_n}{\gamma_0 + \gamma_n} \qquad (\mu *_r = 1) \tag{13}$$

$$T_n = \begin{pmatrix} e^{-\gamma_n d} & 0 \\ 0 & e^{\gamma_n d} \end{pmatrix} \quad \text{n=a or b} \tag{14}$$

Γ_n: the reflection coefficient at the Air Material interface.

T_n: the transmission matrix of a line of length d.

$$\text{or : } \gamma_0 = j\frac{2\pi}{\lambda_0}\sqrt{1-\left(\frac{\lambda 0}{\lambda c}\right)^2} \tag{15}$$

$$\text{and } \gamma_n = j\frac{2\pi}{\lambda_0}\sqrt{\varepsilon *_{rn}\,\mu *_{rn} - \left(\frac{\lambda_0}{\lambda_c}\right)^2} \tag{16}$$

with $n = a$ or b

γ_0 and γ_n : the propagation constants in the air and in the dielectric respectively.

λ_c and λ_0 :the cut-off wavelength of the rectangular waveguide and the free space wavelength respectively.

$\varepsilon *_{ra}$ and $\varepsilon *_{rb}$ are the complex permittivity of the reference and MUT samples, respectively.

The matrix product $M_aM_b^{-1}$ eliminates the influence of the two error ports on the device parameters as shown in relation (17):

$$M_a M_b^{-1} = x.T_{ref_a}.T_a.T_{ref_a}^{-1}.T_{ref_b}.T_b^{-1}.T_{ref_b}^{-1}.x^{-1} \tag{17}$$

where M^{-1} means the inverse of the square matrix M.

Equation (17) shows that $M_aM_b^{-1}$ and $T_{ref_a}\cdot T_a \cdot T_{ref_a}^{-1} \cdot T_{ref_b}\cdot T_b^{-1}\cdot T_{ref_b}^{-1}$ are similar, and have the same trace defined by the sum of the diagonal elements.

$$Tr(M_a M_b^{-1}) = Tr(T_{ref_a}.T_a.T_{ref_a}^{-1}.T_{ref_b}.T_b^{-1}.T_{ref_b}^{-1}) \tag{18}$$

with Tr (M) is the trace of the square matrix (M).

The relation (18) is a nonlinear equation whose only unknown is the permittivity complex ε^*_{rb} of the material under test.

Either:

$$f(\varepsilon_{rb}*) = Tr(T_{ref_a}.T_a.T_{ref_a}^{-1}.T_{ref_b}.T_b^{-1}.T_{ref_b}^{-1}) \tag{19}$$

f is a function of $\varepsilon *_{ra}$, λ_0, $\lambda_c$and d where $\varepsilon *_{rb}$ is the single unknown. Many complex values of $\varepsilon *_{rb}$ can satisfy the function f. If a good initial value of $\varepsilon *_{rb}$ is available, the resolution function f iteratively leads directly to the true value of $\varepsilon *_{rb}$ .This technique based on the cascade wave matrix (WCM) makes it possible to mathematically eliminate the matrices of errors x and y and to extract a nonlinear equation whose resolution can be done in an iterative manner via an algorithm of resolution. Equation (18) can be simplified if the air is taken as the reference dielectric during the first compute,then: $\varepsilon_{ra}* = 1$, $\gamma_a = \gamma_0 \rightarrow$ and $\Gamma_a = 0$.

Equation (18) becomes:

$$Tr(M_a M_b^{-1}) =$$

$$Tr(T_a.T_{ref_b}.T_b^{-1}.T_{ref_b}^{-1}) = 2\frac{\Gamma_b{}^2\cosh(\Lambda_a) - \cosh(\Lambda_b)}{\Gamma_b{}^2 - 1} \tag{20}$$

or: $\Lambda_a = (\gamma_0 + \gamma_2)d$ and $\Lambda_b = (\gamma_0 - \gamma_2)d$

3. RESULTS AND DISCUSSION

First, we are interested in the filling rate effect of TiC inclusions, and contrast on the effective permittivity of the Al_2O_3-TiC composite material.The results were obtained by simulations of the unit cell of the composite material in a three dimensional 3D as shown in Figure 1 using electromagnetic simulation software.We perform simulations for a dielectric alumina matrix with permittivity and relative permittivity of spherical inclusions equal to 13.5; 27; 90 and 270. Four contrasts $K = \frac{\varepsilon_2}{\varepsilon_1} = \frac{13.5}{9}, \frac{27}{9}, \frac{90}{9} et \frac{270}{9}$ were analyzed by changing the volume fraction f of the spherical inclusions of radius R = 50 μm incorporated in the matrix from 0.8% to 80%. The inclusions are in permanent contact without any overlap. In all simulations, the phases are initially discharged and no longer contain free charges. The external electric field is applied in the direction (Oz).

Figure 3 shows the variation of the effective dielectric permittivity as a function of the contrast of permittivity k and of the volume fraction f of the TiC inclusions.

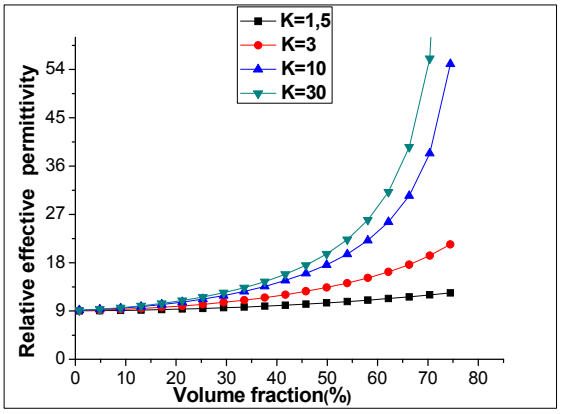

Figure 3: Evolution of the effective Permittivity depending on the volume fraction of Al_2O_3-TiC composite for different permittivity contrasts k

The results of the simulations are compared with the different classical mixing laws for different contrasts in Figure 4.

The results show that the effective permittivity ε_{eff} of the composite studied depends on both the volume fraction f and the permittivity contrast K between the inclusions and the matrix. Figure 3 indicates that for the low filling rate of TiC inclusions from 0.8% to 15%, the effective permittivity is approximately constant for all contrasts. It then increases with the increase in contrast and filling rate of TiC inclusions from 15%. This is due to the increase in the filling rate that influences the distance between the spherical inclusions which dec-

reases, then the percolation threshold of the composite material decreases, this means that the conductivity of the material is improved [12].

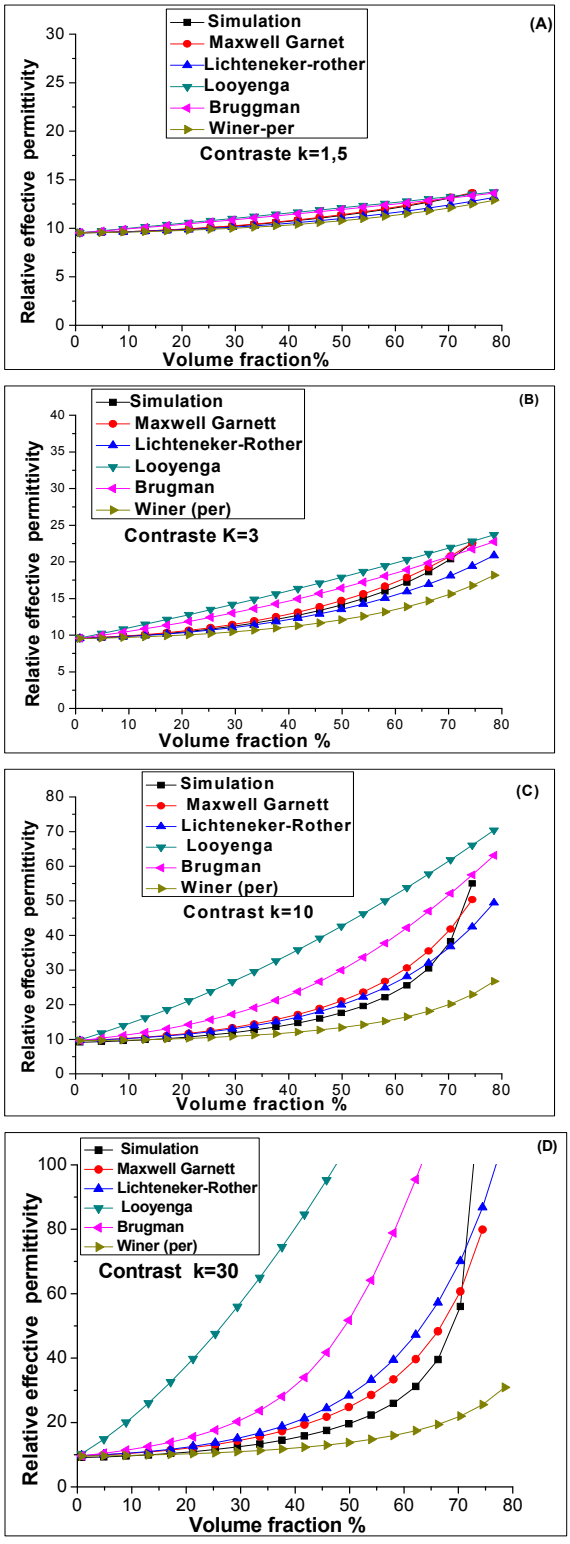

Figure 4: Comparison of the simulation results with the mixing laws for different contrasts: (A) for K = 1.5, (B) for K = 3, (C) for K = 10 and (D) for K = 30.

Therefore, the effective permittivity increases. For K≤3, the Maxwell-Garnett law is more suitable for predicting with more precision the effective permittivity of the composite over the entire studied interval. This is due to the formulation of this model which is based on the assumption that the inclusions are assumed to be spherical, isolated, without interactions and immersed in a homogeneous matrix. For volume fractions higher than 30% and k>3, this law is unable to estimate the effective permittivity. For low contrasts k≤1.5, the results of the simulations and mixing laws are very close and quasi-linear across the entire interval of the volume fraction. If the mixture is diluted, below 30% and K> 1.5, the laws of Lichtenecker-Rother and Winer allow to estimate the effective permittivity. On the other hand, the laws of Looyenga and Bruggeman are unable to estimate the effective permittivity even for small volume fractions and contrasts. We note a divergence between the simulation results and the mixing laws for high volume fractions and contrasts (K≥10). This behavior is mainly due to the interactions between the inclusions which become very significant at high concentration [16].

Figures 5 and 6 illustrate the frequency evolution of the complex dielectric permittivity ε^* for the three ceramic composites Al_2O_3-TiC, Al_2O_3-0.3TiC and Al_2O_3-0.7TiC across the two bands X and Ku.

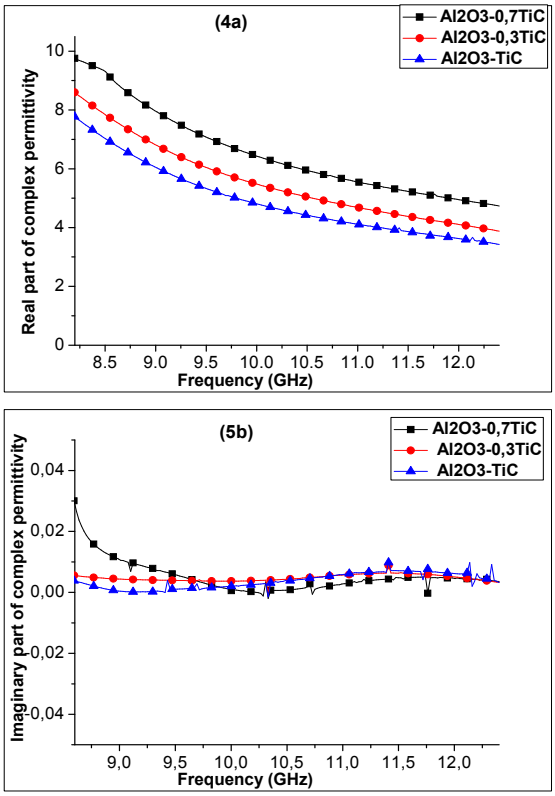

Figure 5: Frequency evolution of the real part (5a) and imaginary part (5b) of the complex permittivity of the composites studied in the X band

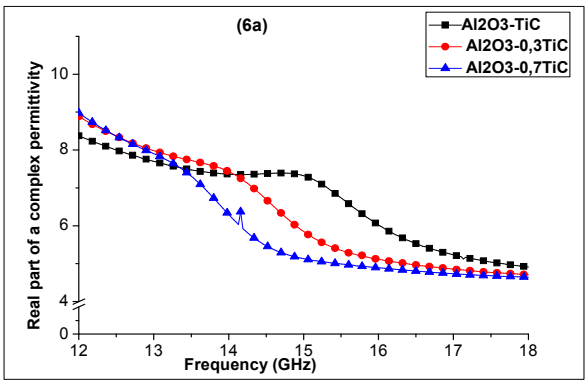

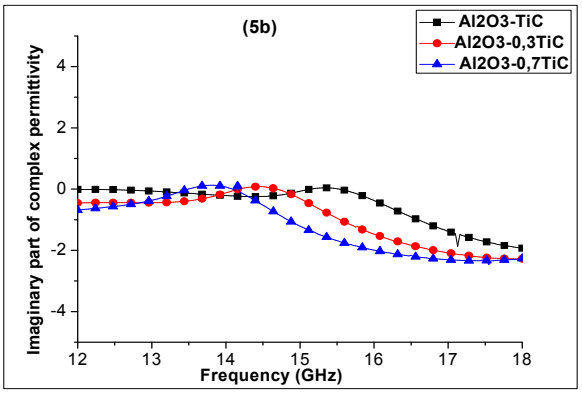

Figure 6: Frequency evolution of the real part (6a) and imaginary part (6b) of the complex permittivity of the composites studied in the Ku band.

The results show that the values of the real □□ and imaginary □□□ parts of the complex permittivity □* are generally high for the composite filled with 70% of TiC. This indicates that the addition of TiC particles can effectively improve the parameters of the complex permittivity of the composite material. These results also indicate that the evolution of the complex permittivity of the three samples depends on the frequency. The curves 5a and 6a of the real part of the permittivity for the three composites in the two bands are decreasing as a function of the frequency. While a small variation of the imaginary part as a function of the frequency is observed when the frequency increases from 8 GHz to 14 GHz. This means that there is a low dielectric loss in the composites in the X band and in the frequency range from 12 GHz to 14 GHz. Beyond 14 GHz, the imaginary part of the complex permittivity decreases and takes negative values. These results indicate the existence of dielectric losses in the composites studied for the high frequencies. This behavior is due to the relaxation losses of the polarization by the hysteresis between the displacement current and the accumulation potential when the frequency increases [23]. The results obtained in this work are in good agreement with the literature [24].

4. CONCLUSION

In this work, we adopted the Transmission / Reflection method by rectangular waveguide. The objective is to extract the complex permittivity of the Al_2O_3-TiC composite over a wide frequency band. The results obtained demonstrate that the effective permittivity increases together with the increase in the filling rate of the TiC inclusions and with the increase in the contrast K between the inclusions and the matrix. We also note that the results obtained prove that the real parts of the complex permittivity decrease simultaneously with the frequency increase in both X and Ku bands. While the imaginary parts of the complex permittivity are almost constant in the X band and take negative values in the Ku band. The dielectric properties of the composites studied in this research affirm that the latter are good microwave absorbents.

REFERENCES

[1] Dinulović, M., Rašuo, B.: Dielectric modeling of multiphase composites, Composite Structures, Elsevier,Vol. 93, No. 12, pp.3209-3215, 2011.

[2] Dinulović, M., Rašuo, B.: Dielectric properties modeling of composite materials, FME Transactions, Vol. 37, No .3, pp. 113-118, 2009.

[3] Ozturk, S., Kong,F., Singh,R.K., Kuzy,J.D., Li,C.,and Trabelsi,S.: Dielectric properties, heating rate, and heating uniformity of various seasoning spices and their mixtures with radio frequency heating, Journal of Food Engineering,Vol.228, pp. 128-141,2018.

[4] Galindo-Romera, G., Carnerero-Cano, J., Martınez-Martınez, J. J., and Herraiz-Martınez, F. J.: An IoT Reader for Wireless Passive Electromagnetic Sensors 2017,Vol.17,No.4, 693,2017.

[5] Ozturk, M., Akgol, O., Sevim, U.K., Karaaslan, M., Demirci, M., and Unal, E.: Experimental work on mechanical, electromagnetic and microwave shielding effectiveness properties of mortar containing electric arc furnace slag, Constr. Build. Mater, Vol. 165, pp. 58-63, 2018.

[6] Janezic, M.D., Jarvis, J.B.: Full-Wave Analysis of a Split-Cylinder Resonator for Nondestructive Permittivity Measurements, IEEE Transactions on microwave theory and techniques, Vol. 47, No .10, 1999.

[7] Friedsam, G., Biebl, E.: A broadband free-space dielectric properties measurement system at millimeter wavelengths, IEEE Transaction on instrumentation and measurement, Vol.46, No.2, pp. 515-518, 1997.

[8] Jarvis, J.B., Janezic, M., Riddle, B., Johnk, R., Kabos, P., Holloway, C., Geyer, R., Grosvenor, C.: Measuring the Permittivity and Permeability of Lossy Materials: Solids, Liquids, Metals, Building Materials, and Negative-Index Materials, NIST Technical note 1536 ,2004.

[9] Sharma, K., Agili, SS., Morales, AW.: Wideband Dielectric Characterization of 3-D Printable Triethylene Glycol Dimethacrylate Ester Plastic, IEEE Transactions on Instrumentation and Measurement , Vol.68,No. 11 ,pp. 4419-4426 ,2019.

[10] Charles, M., Ahmad Hawad, N.: « Propriétés électromagnétiques matériaux par la mesure des paramètres S sur ligne de transmission » ,18th International Congress of Metrology, No. 07010, 2017.

[11] Ghodgaonkar, D. K., Varadan, V. V., Varadan, V. K.: A Freespace Method for Measurement of Dielectric Constants and Loss Tangents at Microwave Frequencies, IEEE Trans. Instrum. Meas, Vol. 38, pp.789–793, 1989.

[12] Wang, Y., Lou, F., Zhou, W.C. Zhu. D.M.: Dielectric and Microwave Absorption Properties of TiC-Al_2O_3/Silica Coatings at High Temperature, Journal of electronic materials, Vol. 46, No. 8, 2017.

[13] Zhang, Y., Wang, L., Jiang, W., Chen, L., Bai, G.: Microstructure and properties of Al2O3– TiC nanocomposites fabricated by spark plasma sintering from high-energy ball milled reactants, J. Eur. Ceram. Soc, Vol.26, No .15, pp 3393–3397, 2006.

[14] Zhou, XF. Jia, ZR. Feng, AL., Wang, XX. Liu, JJ. Zhang, M., and al.: Synthesis of fish skin-derived 3D carbon foams with broadened bandwidth and

excellent electromagnetic wave absorption performance, Vol.152, pp.827-836, 2019.

[15] Wang, Y., Luo, F., Zhou,WC., Zhu, DM.: Dielectric and electromagnetic Wave absorbing properties of TiC/epoxy composites in the GHz range, Ceramics International,Vol.40 ,pp. 10749-10754, 2014.

[16] Elboubakraoui, M. C., Bri, S., Foshi, J.: Dielectric Properties of SiCf/SiC Composites, FME Transactions, Vol. 46, 86-92, 2018.

[17] Jylhä, L., Sihvola, A. "Numerical modeling of disordered mixture using pseudorandom simulations'', IEEE Transactions on Geoscience and Remote Sensing, Vol. 43, No.1, pp. 59-64, 2005.

[18] J. Chaskalovic, "Méthode des éléments finis pour les sciences de l'ingénieur", Tec et Doc – Lavoisier, 2004.

[19] Jebbor, N., Bri, S.: Effective Permittivity of Periodic Composite Materials; Numerical Modeling by the Finite Element Method, J. Electrostat, Vol. 70, No. 4, pp. 393-399, 2012.

[20] Zhao, X., Wu, Y., Fan, Z., Li, F.: Threedimensional simulations of the complex dielectric properties of random composites by finite element method, J. Appl. Phys, Vol. 95 , No. 12, pp. 8110-8117, 2004.

[21] Jebbor, N., Bri, S., Sánchez, A.M., Chaibi, M.: Afast calibration-independent method for complex permittivity determination at microwave frequencies, Measurement, Vol. 46, pp. 2206-2209, 2013.

[22] Hasar, U.C.: "Determination of full S-parameters of a low-loss two-port device from uncalibrated measurements", review of scientific instruments, Vol .89, No.12, 124701, 2018.

[23] Han, T. et al.: Effect of SiC nanowires on the high temperature microwave absorption properties of SiCf/SiC composites, Journal of the European Ceramic Society, Vol.39,pp. 1743–1756 , 2019.

[24] Shao, T., et al.: High temperature absorbing coatings with excellent performance combined Al_2O_3 and TiC,Journal of the European Ceramic Society, Vol.40, pp. 2013–2019, 2020.

NOMENCLATURE

TiC	Titanium carbide
Al_2O_3	Alumina
Al_2O_3-TiC	Alumina titanate
ε_{eff}	Effective permittivity
f	Volume fraction
S_{ij}	Scattering parameters
ε_1	Permittivity of the matrix
ε_2	Permittivity of the inclusion
K	Contrast of permittivity
T/R	Transmission / Reflection method
FE	Finite element method
Γ	Reflection coefficient
T	Transmission matrix
γ	Propagation constant
λ	Wavelength

ДИЕЛЕКТРИЧНЕ КАРАКТЕРИСТИКЕ КЕРАМИЧКИХ КОМПОЗИТНИХ МАТЕРИЈАЛА СА МЕТАЛНОМ МАТРИЦОМ НА БАЗИ АЛУМИНИЈУМА ОЈАЧАНОМ ТИТАНИЈУМ КАРБИДОМ

Ј. Оухасан, С. Бри, М.К. Ел Боубакраоуи, М. Хабиби

Истражују се диелетричне и микроталасне карактеристике три керамичка композита Al_2O_3-TiC, Al_2O_3-0.3TiC и Al_2O_3-0.7TiC. Добијени резултати показују да се ефективна пермитивност повећава са порастом стопе пуњења титанијум карбидом. Конвенционални закони мешања омогућавају процењивање пермитивности за мале запреминске фракције и контрасти. Вредности реалног дела комплексне пермитивности опадају са порастом фреквенција у два опсега X и Ku, док је имагинарни део приближно константан у опсегу X а добија негативне вредности у опсегу Ku.